Human Coherence from First Principles

Balanced Exchange, Hyperbolic Cost, and Finite-Temperature Alignment on the Recognition Ledger

Jonathan Washburn

Recognition Physics Institute, Austin, Texas

jon@recognitionphysics.org

Abstract

Ask what it means for a person to be coherent and the usual answers are a feeling or a fragile wave. Neither is a physical definition, and neither says what to measure. We develop a quantitative account of human coherence on the recognition ledger, where every directed bond carries a positive ratio x, deviation from balance costs $J(x) = \frac{1}{2}(x + x^{-1}) - 1 = \cosh \varepsilon - 1$ ($\varepsilon = \ln x$), and an account's skew is its outgoing minus its incoming log-ratio. All mathematical results follow unconditionally from J and boundary balance; their reading as statements about human timing rests on four explicit working identifications (Premises P1–P4). Cost alone never reduces coherence. Six quantitative consequences follow. First, the wasted cost paid above the even way of carrying the same total exchange brackets coherence loss from both sides inside the no-wrap lag window (up to the bounded curvature factor $\cosh B_{\max}$): coherence is thrift, not calm. Second, for a single account under the canonical cosh-Gibbs weight, the exact signed coherence is the modified Bessel ratio $K_{iq}(a)/K_0(a)$, whose variance obeys $(a + \frac{1}{2})^{-1} < V(a) < a^{-1}$ and whose fourth cumulant is strictly negative at every stiffness. Third, between two people total cost factorizes via the composition law of J into throughput and skew, coherence depends on skew alone, and by shared-bond reciprocity both parties carry the exact same burden and coherence curve regardless of who is ahead. Fourth, unresolved skew carried across channels of unequal series depth separates their settled log-ratios up to a universal ceiling $\ln(a_k/a_j)$ while total burden grows exponentially as $e^{|\sigma|/M}$; a quadratic penalty produces neither. Fifth, in the exact finite-temperature two-account ensemble, raising skew separates subsystem means while exponentially narrowing fluctuations within each channel, so total pooled variance can fall under load. Sixth, a zero-net-flow outside rhythm cannot erase boundary skew; it can hold alignment only by paying a strict holding excess above the separated minimum. Four explicit identifications separate the mathematical laws from physiological measurement, and three prospective experimental protocols—with explicit power analyses against the quadratic rival—specify how to test the hyperbolic law in the large-excursion regime.

1 Introduction

Human coherence is usually described in one of two ways: as a subjective feeling of calm or autonomic "flow" [6], or as a delicate macroscopic quantum wave that warm tissue is somehow supposed to preserve. The feeling cannot be calculated from physics, and a fragile quantum superposition does not survive room-temperature water. Meanwhile, physiological studies of cardiorespiratory phase synchronization [5], paced breathing [6], and allostatic load [7] measure rich alignment phenomena, yet lack a single exact cost functional linking multi-channel synchronization, stress-induced rigidity, and interpersonal balance.

Recognition Science begins from a smaller, harder starting point: distinguishable occurrences exist, comparing two occurrences requires information from both, and examining an earlier record is a new occurrence [16]. On the resulting recognition ledger, a person is modeled as a finite boundary—a set of accounts joined internally and to the world by directed bonds. Every bond carries a positive comparison ratio $x > 0$ (or signed log-ratio $\varepsilon = \ln x$), and every bond turns along its recognition cycle at a pace set by its state. *A person is coherent when all of their bonds turn at one pace while carrying active, closed-book exchange.*

The mathematical theorems below are exact consequences of convex analysis and statistical mechanics for the canonical comparison cost $J(x) = \frac{1}{2}(x + x^{-1}) - 1 = \cosh \varepsilon - 1$, whose uniqueness under reciprocal composition and calibration is proved elsewhere [1, 2, 3]. Reading these laws as statements about human physiology is explicitly conditional on four working identifications (Premises P1–P4). Six concrete consequences follow, several overturning standard quadratic intuition:

1. **Coherence is thrift, not calm.** Standing cost alone does not destroy coherence; spread in turn rate does. Within the no-wrap lag window, the excess cost paid above the cheapest even allocation of the same total exchange brackets coherence loss from both sides up to $\cosh B_{\max}$ (Theorem 1). High intensity at one pace loses nothing; two zero-net-throughput bonds pulling opposite ways drop to $|W| = 0$ periodically.

2. **Hyperbolic locking and strict platykurtosis.** Under the canonical cosh-Gibbs weight $p_a(x) \propto e^{-a \cosh x}$ (Premise 4), the exact signed coherence is the modified Bessel ratio $H_a(q) = K_{iq}(a)/K_0(a)$. Its variance is strictly clamped below $1/a$ and its fourth cumulant is strictly negative at every stiffness $a > 0$ (Theorem 2), generating high-lag sign reversals absent from Gaussian and exponential noise.

3. **Boundary charge and symmetric pair loss.** Skew is a boundary charge: it sums to zero over any closed network, and nothing done inside a person changes their net boundary skew (Theorem 3). On a reciprocal pair, total cost factorizes identically through the composition law of J into throughput and skew, skew and throughput multiply, coherence depends on skew alone, and shared-bond reciprocity forces both sides to carry the exact same burden and dimming curve (Theorem 4).

4. **Unresolved skew hits a ceiling in spread and explodes in burden.** When a boundary carries net skew across channels of unequal series depth a_k, shallow channels absorb load first and separate from deep channels, but their log-ratio gap stays strictly below $\ln(a_k/a_j)$ while total burden climbs exponentially as $e^{|\sigma|/M}$ (Theorem 5). Quadratic homeostasis predicts an unbounded linear gap and polynomial cost.

5. **At finite temperature, stress can lower total variance.** Solving the two-account fixed-skew Gibbs ensemble in closed form shows two opposing forces: subsystem means pull apart toward $\ln(b/a)$ while fluctuations inside each channel freeze exponentially (Theorem 7). For moderate stiffness contrast, total pooled variance actually drops as skew increases (Theorem 9): stress-induced hyper-rigidity coexists with rising setpoint separation.
6. **Living coherence is active, and zero-net-flow rhythms pay a holding price.** An uncompensated standing skew exhausts any finite reserve in logarithmic time (Theorem 10). A zero-net-flow outside rhythm cannot remove boundary skew; it can hold equal pace only by paying a strictly positive holding excess above the separated minimum, so any cost-decreasing relaxation returns a skewed boundary to separated paces once the drive stops (Theorem 11).

Four explicit physical identifications connect the ledger's mathematics to human measurements: that a bond's turn rate reads its log-ratio, that a person is a composite boundary with channels of unequal depth, that coherence averages over the boundary's bonds, and that the interior settles near least burden with flat log-ratio Gibbs fluctuations. We state each premise where it enters, identify a decisive clock-readout fork (log-ratio versus marginal burden), and specify three prospective experimental protocols with explicit power calculations against the quadratic rival.

2 The Recognition Ledger and Modeling Premises

2.1 Accounts, bonds, cost, and skew

Consider a finite directed bond ledger $L = (V, E, \mathrm{src}, \mathrm{dst}, x)$, where V is a finite set of accounts, E is a finite set of directed bonds (assumed loopless, or counting each endpoint incidence separately), each bond $b \in E$ runs from $\mathrm{src}(b) \in V$ to $\mathrm{dst}(b) \in V$, and each bond holds a positive comparison ratio $x_b > 0$. Write the signed log-flow as $\varepsilon_b = \ln x_b \in \mathbb{R}$.

In Recognition Science, the canonical dimensionless comparison cost is uniquely fixed by reciprocal symmetry $J(x) = J(x^{-1})$, the d'Alembert composition law on multiplicative ratios, continuity, and unit curvature at balance $J''(1) = 1$ [1, 2, 3]:

$$J(x) = \frac{x + x^{-1}}{2} - 1 = \frac{(x-1)^2}{2x}, \qquad J(e^{\varepsilon}) = J_{\log}(\varepsilon) := \cosh \varepsilon - 1. \tag{1}$$

Three exact properties govern everything that follows: $J(x) \geq 0$ with equality if and only if $x = 1$ ($\varepsilon = 0$); reciprocity symmetry $J(x) = J(x^{-1})$ ($J_{\log}(-\varepsilon) = J_{\log}(\varepsilon)$); and the d'Alembert composition identity

$$J(gr) + J(g/r) = 2J(g) + 2J(r) + 2J(g)J(r) \qquad (g, r > 0). \tag{2}$$

For any account $i \in V$, define its incident bonds $E(i) = \{b \in E : \mathrm{src}(b) = i \text{ or } \mathrm{dst}(b) = i\}$, its *burden* $C_i = \sum_{b \in E(i)} J_{\log}(\varepsilon_b)$, and its *net reciprocity skew*

$$\sigma_i := \sum_{b\colon \mathrm{src}(b)=i} \varepsilon_b - \sum_{b\colon \mathrm{dst}(b)=i} \varepsilon_b. \tag{3}$$

An account has *closed books* (admissibility) when $\sigma_i = 0$. Positive σ_i denotes net outgoing log-flow (extraction); negative σ_i denotes net incoming log-flow (contribution), matching the signed boundary-ledger conventions of [17]. A ledger is *balanced* when every ratio equals one ($\varepsilon_b = 0$ for all b).

2.2 Explicit premises connecting the ledger to human timing

Every mathematical theorem in Sections 3–8 holds identically for arbitrary positive stiffnesses $a, a_k > 0$ and gain $\nu \neq 0$ without fitting biological data. To read those theorems as statements about human physiological observables, we isolate four working identifications once so their exact scope stays visible throughout.

Premise 1 (Turn-rate readout, P1)**.** Each bond b advances its recognition phase at angular rate $\theta_b = \theta_0 + \nu\varepsilon_b$, with a common rest pace θ_0 and nonzero linear gain ν across the compared ensemble.

All strict-positivity conclusions require only that θ_b be a common strictly monotone function of ε_b. In Section 6 we explicitly analyze the alternative *marginal-burden readout* $\theta_b = \theta_0 + c\, a_b \sinh \varepsilon_b$, where the pace-separation effect vanishes even though log-ratios still separate. The scale ν is not derived here, so dimensionless lags $q = \nu t$ appear in place of seconds.

Premise 2 (Composite human boundary, P2)**.** A human being is represented on the ledger by a finite subset of accounts $S \subset V$, connected internally and exchanging with the exterior $V \setminus S$ through $M \geq 2$ channels of unequal series depth $a_1, \ldots, a_M > 0$.

Premise 3 (Boundary bond ensemble, P3)**.** The coherence of a boundary is evaluated over its active bond ensemble with probability weights $p_b > 0$ ($\sum_b p_b = 1$), via the characteristic function (Kuramoto-type order parameter of free-running turn rates [4]) $W(t) = \sum_b p_b e^{i\theta_b t}$.

Premise 4 (Least-burden interior and cosh-Gibbs fluctuations, P4)**.** For a fixed boundary net skew σ_S, the deterministic baseline of the interior minimizes total channel burden, and finite-temperature fluctuations follow the canonical Gibbs weight $e^{-\sum_k a_k \cosh \varepsilon_k}$ with respect to the flat log-ratio volume $d\varepsilon = dx/x$ (effective inverse temperature folded into the positive stiffnesses a_k).

Premise 4 enters in Sections 4, 6, 7, 8.3, and 9. Theorems 1, 3, 4, 10, and the incident burden floors do not use Premise 4. Specific physiological coordinate maps (such as respiratory or cardiac timings) are candidate realizations tested prospectively in Section 9, not axioms.

3 Coherence Is Agreement of Pace, and Coherence Is Thrift

3.1 Why cost alone does not decay coherence

Given any finite ensemble Ω with probability weights $p_i \geq 0$ ($\sum_i p_i = 1$) and turn rates $\theta : \Omega \to \mathbb{R}$, the ensemble coherence at lag t is the weighted phase average

$$W(t) := \sum_{i \in \Omega} p_i e^{i\theta_i t}. \tag{4}$$

Setting $\bar{\theta} = \sum_i p_i \theta_i$ and centering in the rotating frame, $W_c(t) = e^{-i\bar{\theta}t} W(t)$, preserves the modulus $|W_c(t)| = |W(t)|$.

A naive exponential bridge $W(t) = e^{-C}$ between standing cost and coherence is mathematically false. Whenever all turn rates agree ($\theta_i = c$ for all i), $W(t) = e^{ict}$ and $|W(t)| = 1$ regardless of how large the standing costs C_i are. Conversely, on a general two-state ensemble with equal weights $p_1 = p_2 = \frac{1}{2}$ and turn rates 0 and π at zero standing cost (prior to imposing Premise 1), $W(1) = 0$ despite zero cost. What governs coherence loss is the *variance of turn rates*, $\mathrm{Var}_p(\theta) = \sum_i p_i(\theta_i - \bar{\theta})^2$:

$$\frac{2}{\pi^2} t^2 \,\mathrm{Var}_p(\theta) \;\le\; 1 - \mathrm{Re}\, W_c(t) \;\le\; \frac{1}{2} t^2 \,\mathrm{Var}_p(\theta), \tag{5}$$

where the upper bound holds globally for all $t \in \mathbb{R}$ and the lower bound holds throughout the no-wrap window $|(\theta_i - \bar{\theta})t| \le \pi$ (outside which $W_c(t)$ can revive periodically). Whenever a fourth moment exists, the global lower bound $1 - \mathrm{Re}\, W_c(t) \ge \frac{1}{2} t^2 \mathrm{Var}_p(\theta) - \frac{1}{24} t^4 \mathbb{E}_p[(\theta - \bar{\theta})^4]$ also holds without any window restriction.

3.2 The thrift bracket

Under Premise 1, cost enters coherence not through total burden, but through the Jensen gap—the *wasted* burden paid above the even allocation of the same total exchange.

Theorem 1 (Coherence is thrift)**.** *Let Ω be a finite active bond ensemble with strictly positive probability weights $p_b > 0$ ($\sum_b p_b = 1$) and log-flows ε_b satisfying $|\varepsilon_b| \le B_{\max}$. Write the weighted mean $\bar{\varepsilon} = \sum_b p_b \varepsilon_b$, the spread $D = \sum_b p_b (\varepsilon_b - \bar{\varepsilon})^2$, and the wasted cost above the even allocation as $\Delta C := \sum_b p_b J_{\log}(\varepsilon_b) - J_{\log}(\bar{\varepsilon})$. Then:*

1. *$\Delta C \ge 0$, with equality if and only if $\varepsilon_b = \bar{\varepsilon}$ for all $b \in \Omega$.*
2. *The wasted cost brackets the spread from both sides:*

$$\frac{1}{2} D \;\le\; \Delta C \;\le\; \frac{\cosh B_{\max}}{2} D. \tag{6}$$

3. *Under Premises 1 and 3, coherence loss is bracketed by wasted cost:*

$$\frac{4}{\pi^2} \frac{(vt)^2}{\cosh B_{\max}} \Delta C \;\le\; 1 - \mathrm{Re}\, W_c(t) \;\le\; (vt)^2 \,\Delta C, \tag{7}$$

with the upper bound holding for all $t \in \mathbb{R}$ and the lower bound valid inside the no-wrap window $|v(\varepsilon_b - \bar{\varepsilon})t| \le \pi$.

Proof. For any $x, y \in \mathbb{R}$, integrating $\cosh''(u) = \cosh u \ge 1$ twice yields the exact lower tangent bound

$$\cosh y - \cosh x - \sinh x \cdot (y - x) \;\ge\; \frac{(y - x)^2}{2}.$$

Similarly, whenever $|x|, |y| \le B_{\max}$, $\cosh u \le \cosh B_{\max}$ on the closed interval between x and y, giving

$$\cosh y - \cosh x - \sinh x \cdot (y - x) \;\le\; \frac{\cosh B_{\max}}{2} (y - x)^2.$$

Since $|\bar{\varepsilon}| \le \sum_b p_b|\varepsilon_b| \le B_{\max}$, set $x = \bar{\varepsilon}$ and $y = \varepsilon_b$, multiply by p_b, and sum over b. The linear term $\sinh\bar{\varepsilon}\sum_b p_b(\varepsilon_b - \bar{\varepsilon})$ vanishes identically, leaving $\Delta C = \sum_b p_b[\cosh\varepsilon_b - \cosh\bar{\varepsilon} - \sinh\bar{\varepsilon}\,(\varepsilon_b - \bar{\varepsilon})]$ and proving (6). Chaining (6) with (5) under $\mathrm{Var}_p(\theta) = v^2 D$ yields (7). □

Note the exact scope of (7): the lower constant carries $(\cosh B_{\max})^{-1}$, which narrows exponentially at extreme excursions, and at lags beyond the no-wrap window $|W_c(t)|$ can revive periodically even while $\Delta C > 0$. Within the operating window, however, $\Delta C = 0 \iff D = 0 \iff |W(t)| \equiv 1$. For equal weights on N bonds carrying total log-flow $T = \sum_{b=1}^{N} \varepsilon_b$, the cheapest even cost is $C_{\mathrm{even}}(T) = N(\cosh(T/N) - 1)$ and (6) reads $\frac{N}{2}D \le C - C_{\mathrm{even}}(T) \le \frac{N}{2}\cosh(B_{\max})D$. A person operating at ten times the intensity loses zero coherence if every bond runs at the shared pace; two equal-weight bonds with zero net throughput carrying equal and opposite log-flows $\pm\sigma/2$ have $T = 0$, $\Delta C = \cosh(\sigma/2) - 1 > 0$, and drop to $|W| = 0$ at $t = \pi/(v|\sigma|)$ (and at odd multiples thereafter).

4 Single-Account Hyperbolic Locking and the Bessel Envelope

Before coupling multiple accounts, consider a single account whose log-imbalance $X \in \mathbb{R}$ is drawn from the canonical cosh-Gibbs weight (Premise 4) with flat log-ratio volume $dx = dr/r$ and stiffness $a > 0$:

$$p_a(x) = \frac{e^{-a\cosh x}}{2K_0(a)}, \qquad x \in \mathbb{R}, \tag{8}$$

where $K_z(a) = \frac{1}{2}\int_{\mathbb{R}} e^{-a\cosh x + zx}\,dx$ is the modified Bessel function of the second kind [8]. Under a linear quasi-static clock detuning $q = vt$ (Premise 1), the exact signed coherence is

$$H_a(q) := \mathbb{E}_a[e^{iqX}] = \frac{K_{iq}(a)}{K_0(a)}, \qquad W(t) = e^{i\theta_0 t}H_a(vt). \tag{9}$$

Double-exponential tails justify differentiating $K_z(a)$ with respect to its order z on all compact sets. Because p_a is strictly positive and even, $H_a(q)$ is real, even, strictly less than 1 for all $q \neq 0$, and Bochner positive-definite: $\sum_{j,k} c_j\bar{c}_k H_a(q_j - q_k) = \mathbb{E}_a|\sum_j c_j e^{iq_jX}|^2 \ge 0$.

Write $V(a) = \mathbb{E}_a[X^2]$, $m_4(a) = \mathbb{E}_a[X^4]$, fourth cumulant $c_4(a) = m_4(a) - 3V(a)^2$, and excess kurtosis $\gamma_2(a) = c_4(a)/V(a)^2$.

Theorem 2 (Hyperbolic locking and universal platykurtosis)**.** *For every stiffness $a > 0$, the cosh-Gibbs law* (8) *satisfies*

$$\frac{1}{a + 1/2} \;<\; V(a) \;<\; \frac{1}{a}, \qquad c_4(a) \;<\; 0. \tag{10}$$

In particular, under (9)*, $1 - H_a(q) \le \frac{1}{2}V(a)q^2 < q^2/(2a)$ for all $q \neq 0$ (strictly tighter than the curvature-matched quadratic dispersion bound, though $H_a(q)$ eventually crosses below $e^{-q^2/(2a)}$ at large q where H_a turns negative), while at sufficiently small nonzero q a variance-matched Gaussian $e^{-V(a)q^2/2}$ exceeds $H_a(q)$ because $\ln H_a(q) = -\frac{1}{2}V(a)q^2 + \frac{1}{24}c_4(a)q^4 + O(q^6)$ with $c_4(a) < 0$.*

Proof. Integration by parts against $p_a'(x) = -a\sinh(x)\,p_a(x)$ (all boundary terms vanish by double-exponential decay) yields three exact identities:

$$a\,\mathbb{E}_a[X\sinh X] = 1, \qquad a\,\mathbb{E}_a[X^3\sinh X] = 3V(a), \qquad a^2\mathbb{E}_a[\sinh^2 X] = a\,\mathbb{E}_a[\cosh X]. \quad (11)$$

Because $x\sinh x > x^2$ for every $x \neq 0$, the first identity immediately gives $aV(a) < a\,\mathbb{E}_a[X\sinh X] = 1$, hence $V(a) < 1/a$. For the lower bound, set $S = a\sinh X$. Since $2(\cosh x - 1) < x\sinh x$ off zero, the third identity gives

$$\mathbb{E}_a[S^2] = a\,\mathbb{E}_a[\cosh X] = a + a\,\mathbb{E}_a[\cosh X - 1] < a + \frac{1}{2}a\,\mathbb{E}_a[X\sinh X] = a + \frac{1}{2}.$$

Applying Cauchy–Schwarz to $1 = \mathbb{E}_a[XS]^2 \le V(a)\,\mathbb{E}_a[S^2]$ gives $V(a) > (a + 1/2)^{-1}$.

For the fourth cumulant, introduce the size-biased probability measure $\tilde{\mathbb{P}}$ with density $(x^2/V(a))\,p_a(x)$. Under $\tilde{\mathbb{P}}$, both X^2 and $h(X) = (\sinh X)/X$ (extended by $h(0) = 1$) are strictly increasing functions of $|X|$, so by the independent-copy covariance identity their covariance is strictly positive:

$$\mathbb{E}_{\tilde{\mathbb{P}}}[X^2 h(X)] > \mathbb{E}_{\tilde{\mathbb{P}}}[X^2]\,\mathbb{E}_{\tilde{\mathbb{P}}}[h(X)].$$

Expanding the definitions of $\tilde{\mathbb{P}}$ gives $V(a)\,\mathbb{E}_a[X^3\sinh X] > m_4(a)\,\mathbb{E}_a[X\sinh X]$. Multiplying by a and substituting (11) yields $3V(a)^2 > m_4(a)$, i.e., $c_4(a) < 0$. □

Three exact asymptotic regimes separate (9) from standard smooth unimodal thermal decoys [9, 11, 12]:

- **Strong stiffness ($a \to \infty$, $u = q/\sqrt{a}$ fixed):** $H_a(\sqrt{a}\,u) = e^{-u^2/2}[1 + (6u^2 - u^4)/(24a) + O(a^{-2})]$, with $V(a) = a^{-1} - (2a^2)^{-1} + O(a^{-3})$ and $\gamma_2(a) = -a^{-1} + O(a^{-2})$ (valid for $a \gg 1$; at $a = 1$ the exact value is -0.3880). Near balance at high stiffness, hyperbolic locking merges smoothly into Gaussian noise.
- **Weak stiffness ($a \downarrow 0$, $L = \ln(2/a)$):** X/L converges in distribution to Uniform$[-1, 1]$, so $H_a(u/L) \to (\sin u)/u$, $V(a) \sim L^2/3$, and $\gamma_2(a) \to -6/5$. At $a = 0.1$, $V = 3.2747$ (threefold tighter than the curvature-matched Gaussian $1/a = 10$) and $\gamma_2 = -0.7549$.
- **Long lag ($q \to +\infty$ at fixed $a > 0$):**

$$H_a(q) = \frac{\sqrt{2\pi/q}\,e^{-\pi q/2}}{K_0(a)}\left[\cos\!\left(q\ln\frac{2q}{a} - q - \frac{\pi}{4}\right) + O_a(q^{-1})\right]. \quad (12)$$

Thus $H_a(q)$ exhibits infinitely many sign reversals of the in-phase signal. Negative lobes are not unique to cosh-Gibbs in isolation—compactly supported boxcar noise (Uniform$[-L, L]$, which is the $a \downarrow 0$ limit above) also oscillates as sinc—but they are completely absent from Gaussian ($e^{-Vq^2/2}$) and exponential/Laplace ($e^{-\gamma|q|}$) thermal decoys, which stay strictly positive everywhere (and the exponential carries a slope cusp at $q = 0$, whereas $H_a'(0) = 0$). At $a = 1$, $V(1) = 0.731100$, $\gamma_2(1) = -0.388024$, the first zero sits at $q = 2.96255$, and H_1 takes the value $H_1(3.5) = -0.011161$ inside its first negative lobe (minimum near $q \approx 3.45$; Figure 1(b)).

5 Two People and Many: Skew as Boundary Charge

5.1 Skew cannot be removed internally

Theorem 3 (Boundary charge conservation). *For any finite directed bond ledger $L = (V, E, \mathrm{src}, \mathrm{dst}, \varepsilon)$ and any subset of accounts $S \subseteq V$,*

$$\sum_{i \in S} \sigma_i = \sum_{\substack{b \in E \\ \mathrm{src}(b) \in S,\, \mathrm{dst}(b) \notin S}} \varepsilon_b - \sum_{\substack{b \in E \\ \mathrm{src}(b) \notin S,\, \mathrm{dst}(b) \in S}} \varepsilon_b. \tag{13}$$

In particular: (i) over the whole ledger, $\sum_{i \in V} \sigma_i = 0$; (ii) internal bonds with both endpoints in S contribute zero to $\sigma_S := \sum_{i \in S} \sigma_i$; and (iii) if $\sigma_S \neq 0$, then both $\sum_{i \in S} |\sigma_i| \geq |\sigma_S|$ and $\sum_{i \notin S} |\sigma_i| \geq |\sigma_S|$.

Proof. Each bond b adds $+\varepsilon_b$ to $\sigma_{\mathrm{src}(b)}$ and $-\varepsilon_b$ to $\sigma_{\mathrm{dst}(b)}$. Summing over $i \in S$ cancels every bond with both endpoints in S, leaves $+\varepsilon_b$ for outgoing cut bonds, and leaves $-\varepsilon_b$ for incoming cut bonds. Taking $S = V$ empties both cut sums. □

Nothing done on a person's internal bonds changes their boundary skew σ_S. Internal rearrangement can move skew from one internal account to another; it can never erase it.

5.2 The two-person pair law

Consider two people A and B joined by a reciprocal pair of bonds: $A \to B$ at ratio $x = e^{\varepsilon_1}$ and $B \to A$ at ratio $y = e^{\varepsilon_2}$. Define the pair's *throughput* $\tau = \varepsilon_1 + \varepsilon_2$, *skew* $\sigma = \varepsilon_1 - \varepsilon_2$ (so $\sigma_A = \sigma$ and $\sigma_B = -\sigma$), geometric mean $g = \sqrt{xy} = e^{\tau/2}$, and imbalance ratio $r = \sqrt{x/y} = e^{\sigma/2}$.

Theorem 4 (Reciprocal pair factorization and coherence). *For a reciprocal pair $(x, y) = (e^{\varepsilon_1}, e^{\varepsilon_2})$ with throughput $\tau = \varepsilon_1 + \varepsilon_2$ and skew $\sigma = \varepsilon_1 - \varepsilon_2$:*

1. ***Factorization (the composition law of J):***

$$C(\tau, \sigma) = J(x) + J(y) = 2 \cosh\frac{\tau}{2} \cosh\frac{\sigma}{2} - 2 = 2J(g) + 2J(r) + 2J(g)J(r). \tag{14}$$

   Thus skew carries an excess burden $C(\tau, \sigma) - C(\tau, 0) = \cosh(\tau/2)\, C(0, \sigma)$ that multiplies *with throughput, whereas a quadratic cost $(\tau^2 + \sigma^2)/4$ separates additively.*

2. ***Reciprocal symmetry of burden:*** *Because A and B share the same two incident bonds and $J(x) = J(x^{-1})$, both accounts carry the exact same incident burden $C_A = C_B = C(\tau, \sigma)$ regardless of who is ahead (so $C_A + C_B = 2C(\tau, \sigma)$ counts each shared bond once per endpoint).*

3. ***Pair coherence reads skew alone:*** *Under Premise 1 with any positive weights $p_1 + p_2 = 1$,*

$$|W(t)|^2 = 1 - 4p_1 p_2 \sin^2\!\left(\frac{v\sigma t}{2}\right), \tag{15}$$

   which equals $|\cos(v\sigma t/2)|^2$ for equal weights. It is completely independent of throughput τ, even in σ, identical across the two-bond ensemble shared by A and B, and equals 1 for all t if and only if $\sigma = 0$.

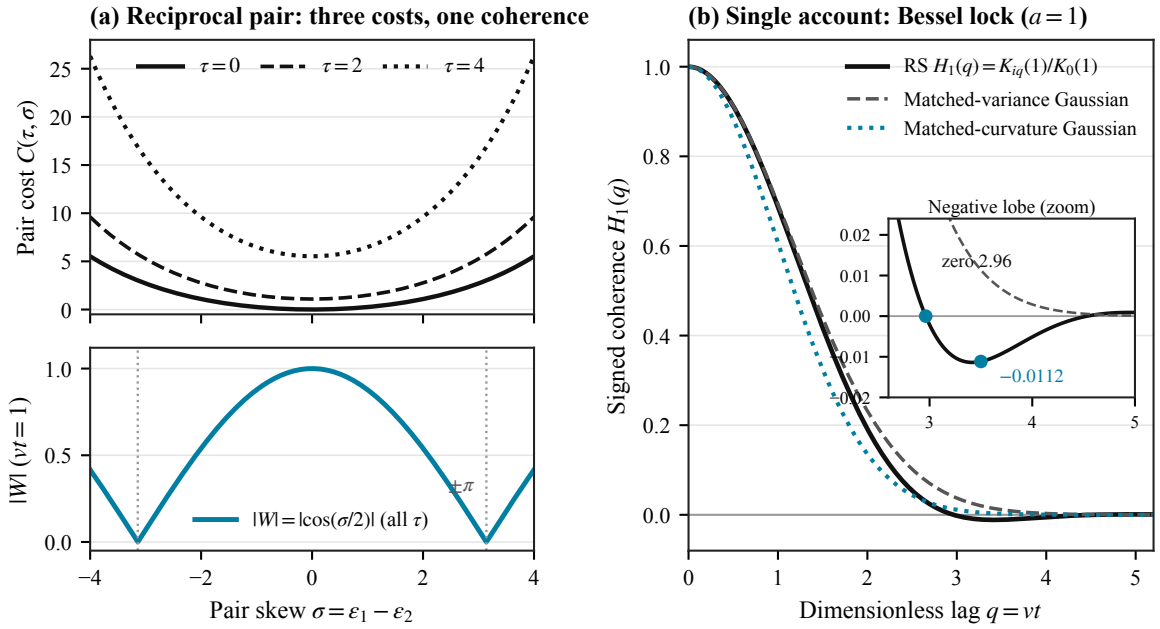


Figure 1. (a) Reciprocal pair: three costs, one coherence. Upper panel: pair cost $C(\tau,\sigma) = 2\cosh(\tau/2)\cosh(\sigma/2) - 2$ for throughputs $\tau = 0, 2, 4$; skew and throughput multiply. Lower panel: equal-weight pair coherence $|W| = |\cos(\sigma/2)|$ at $vt = 1$; all three throughputs collapse onto the same curve, symmetric between the party ahead and the party behind. **(b) Single-account Bessel lock ($a = 1$).** Exact signed coherence $H_1(q) = K_{iq}(1)/K_0(1)$ compared with curvature-matched and variance-matched Gaussian decoys. Inset: the first zero at $q = 2.963$ and negative lobe taking $H_1(3.5) = -0.0112$, absent from Gaussian and exponential decoys.

4. ***Equilibration:*** *Replacing both ratios by their geometric mean* $(x, y) \mapsto (g, g)$ *preserves throughput* τ*, zeroes the pair skew, lowers pair cost by exactly* $2J(r)(1 + J(g))$*, restores* $|W(t)| \equiv 1$*, and leaves every third party's burden unchanged.*

Proof. Write $\varepsilon_1 = \frac{\tau+\sigma}{2}$ and $\varepsilon_2 = \frac{\tau-\sigma}{2}$; applying $\cosh(\alpha+\beta) + \cosh(\alpha-\beta) = 2\cosh\alpha\cosh\beta$ yields (14), which is (2) at (g, r). Subtracting $2J(g)$ gives the exact equilibration saving. Expanding $|p_1 e^{i(\theta_0+\nu\varepsilon_1)t} + p_2 e^{i(\theta_0+\nu\varepsilon_2)t}|^2 = p_1^2 + p_2^2 + 2p_1p_2\cos(\nu(\varepsilon_1 - \varepsilon_2)t)$ and substituting $p_1^2 + p_2^2 = 1 - 2p_1p_2$ and $1 - \cos\phi = 2\sin^2(\phi/2)$ gives (15). □

Figure 1(a) illustrates the separation directly: raising throughput τ from 0 to 4 lifts the pair's zero-skew cost floor from 0 to 5.52 and multiplies every nonzero skew's excess burden by $\cosh(2) \approx 3.76$, while coherence $|W|$ stays locked on the single curve $|\cos(\nu\sigma t/2)|$. Under shared-bond accounting and reciprocity symmetry, the sign of σ records who is owed, not who loses coherence.

5.3 Many people: closed loops, relays, and burden floors

On a general network of many accounts, three structural consequences follow from Theorem 3 and the convexity of $J_{\log}$:

1. **Closed books are circulations.** Every account has $\sigma_i = 0$ if and only if the log-flow

vector lies in the cycle space of the underlying undirected multigraph (a linear combination of uniform signed flows around closed cycles). On a network with no cycles (a forest), closing every book forces $\varepsilon_b = 0$ everywhere: an open living system at zero skew requires closed loops of exchange. Three accounts in a cycle $A \to B \to C \to A$ at one flow ε close all three books even though no individual pair is reciprocal.

2. **Offloading skew onto a third party.** An account A receiving ε from B and sending ε to C has $\sigma_A = 0$ and uniform pace across its two bonds; it is coherent locally, but it carries throughput burden $2(\cosh \varepsilon - 1)$ and leaves $\sum_i |\sigma_i| = 2|\varepsilon|$ undiminished at the endpoints B and C.

3. **Unconditional burden floor.** By convexity of $J_{\log}$, any loopless account i with $d \geq 1$ incident bonds satisfies
$$C_i \;\geq\; d\left(\cosh \frac{\sigma_i}{d} - 1\right) \;\geq\; \frac{\sigma_i^2}{2d}, \tag{16}$$
and any cut of k bonds carrying boundary skew σ_S pays at least $k(\cosh(\sigma_S/k) - 1)$ on the cut bonds alone.

Two simple counterexamples show why *closed books* ($\sigma = 0$) and *one pace* ($D = 0$) are distinct conditions on general networks. One account participating in two balanced reciprocal loops of distinct intensities $e_1 \neq e_2$ has $\sigma = 0$ yet log-flow variance $((e_1 - e_2)/2)^2 > 0$. Conversely, an account with three outgoing bonds all at $\varepsilon = 0.9$ has zero variance ($D = 0$) yet skew $\sigma = 2.7$. Human coherence therefore requires both: closed books *and* uniform pace.

6 One Person, Many Channels: Series Depth, the Ceiling, and Exponential Burden

6.1 How unequal channel stiffnesses arise on the bare ledger

On the bare ledger every single bond costs $J_{\log}(\varepsilon_b)$ and contributes ε_b once to skew. Parallel single-bond channels therefore share skew evenly and produce zero separation. Unequal stiffnesses arise natively without added parameters from *series depth*. Suppose channel k crosses a person's boundary through a serial chain of $a_k \in \mathbb{Z}_{\geq 1}$ bonds whose interior accounts close their own books. By Theorem 3, every bond in the chain carries the same log-flow ε_k; the chain contributes ε_k once to the boundary skew $\sigma = \sum_{k=1}^{M} \varepsilon_k$, while paying $a_k J_{\log}(\varepsilon_k) = a_k(\cosh \varepsilon_k - 1)$. More generally, parallel-series subnetworks or effective multi-bond conduits yield positive real weights $a_k > 0$ (for example, $a_k = 2.5$ corresponds to a balanced two-branch parallel-series conduit of length 5); in all cases a_k scales the channel's comparison burden $a_k(\cosh \varepsilon_k - 1)$ per unit of boundary skew ε_k.

6.2 The heterogeneous channel law and quadratic separator

Under Premise 4, a boundary with $M \geq 2$ channels of heterogeneous positive depths $a_1, \ldots, a_M > 0$ (not all equal) minimizes $C(\varepsilon) = \sum_{k=1}^{M} a_k(\cosh \varepsilon_k - 1)$ subject to $\sum_{k=1}^{M} \varepsilon_k = \sigma$. Compare this directly against standard quadratic homeostasis, which minimizes $C_Q(\varepsilon) =$

$\frac{1}{2}\sum_{k=1}^{M} a_k \varepsilon_k^2$ on the exact same coordinates and constraint, giving $x_k^Q = w_k\sigma$, $C_Q(\sigma) = \sigma^2/(2S_d)$, where $d_k = a_k^{-1}$, $S_d = \sum_j d_j$, and $w_k = d_k/S_d$.

Theorem 5 (Heterogeneous channel law and global quadratic separator)**.** *For any positive depths $a_1, \dots, a_M > 0$ and any boundary skew $\sigma \in \mathbb{R}$, the constrained minimum of $\sum_k a_k(\cosh \varepsilon_k - 1)$ on $\sum_k \varepsilon_k = \sigma$ is unique and given by*

$$a_k \sinh \varepsilon_k^* = \lambda(\sigma), \qquad \varepsilon_k^* = \operatorname{arsinh}\left(\frac{\lambda(\sigma)}{a_k}\right), \qquad C_*(\sigma) = \sum_{k=1}^{M}\left(\sqrt{a_k^2 + \lambda^2} - a_k\right), \tag{17}$$

where $\lambda(\sigma)$ is odd, smooth, and strictly increasing with $\lambda(0) = 0$ and $C_*'(\sigma) = \lambda(\sigma)$. Assume the depths are heterogeneous and $\sigma > 0$. Then:

1. ***Universal log-ratio ceiling:*** *Whenever $a_j < a_k$, $0 < \varepsilon_k^* < \varepsilon_j^*$ and the gap $\varepsilon_j^* - \varepsilon_k^*$ is strictly increasing in σ yet strictly bounded for every finite skew:*

$$0 \;<\; \varepsilon_j^* - \varepsilon_k^* \;<\; \ln\frac{a_k}{a_j}, \qquad \lim_{\sigma\to+\infty}(\varepsilon_j^* - \varepsilon_k^*) = \ln\frac{a_k}{a_j}. \tag{18}$$

2. ***Global majorization separator vs. quadratic homeostasis:*** *At every $\sigma \neq 0$,*

$$0 \;<\; \operatorname{Var}_k(\varepsilon_k^*) \;<\; \sigma^2 \operatorname{Var}_k(w_k), \qquad C_*(\sigma) \;>\; C_Q(\sigma). \tag{19}$$

3. ***Asymptotic exhaustion of shallow buffers and exponential burden:*** *Write $G = (\prod_k a_k)^{1/M}$ and $Q = (G/2)e^{|\sigma|/M}$. As $|\sigma| \to \infty$,*

$$|\lambda(\sigma)| = Q + O(Q^{-1}), \qquad C_*(\sigma) = MQ - \sum_{k=1}^{M} a_k + O(Q^{-1}), \tag{20}$$

the marginal shares $\chi_k = \partial\varepsilon_k^*/\partial\sigma = (a_k^2 + \lambda^2)^{-1/2}/\sum_j (a_j^2 + \lambda^2)^{-1/2}$ flatten from w_k at $\sigma = 0$ to $1/M$ for every channel, and local curvatures $\sqrt{a_k^2 + \lambda^2}$ homogenize to ratio 1.

4. ***Zero-parameter channel invariant:*** *For any two channels at every skew,*

$$\frac{\sinh \varepsilon_j^*}{\sinh \varepsilon_k^*} = \frac{a_k}{a_j} =: s \quad \Longleftrightarrow \quad \varepsilon_j^* = \operatorname{arsinh}(s \sinh \varepsilon_k^*). \tag{21}$$

Proof. Strict convexity and coercivity of $C(\varepsilon)$ ensure a unique minimizer satisfying $a_k \sinh \varepsilon_k^* = \lambda$. Since $\sigma(\lambda) = \sum_k \operatorname{arsinh}(\lambda/a_k)$ has positive derivative $\sum_k (a_k^2 + \lambda^2)^{-1/2}$ and range $\mathbb{R}$, $\lambda(\sigma)$ is smooth, odd, and strictly increasing. Substituting $\cosh(\operatorname{arsinh} u) = \sqrt{1 + u^2}$ gives $C_*(\sigma)$. For $a_j < a_k$ and $\lambda > 0$, $\operatorname{arsinh}(\lambda/a_j) - \operatorname{arsinh}(\lambda/a_k) = \ln(a_k/a_j) + \ln[(\lambda + \sqrt{\lambda^2 + a_j^2})/(\lambda + \sqrt{\lambda^2 + a_k^2})]$, where the second logarithm is strictly negative, strictly increasing in λ, and vanishes as $\lambda \to \infty$, proving (18).

For (19), order $d_1 \geq \dots \geq d_M > 0$. For $\sigma > 0$, the ratio $(\varepsilon_k^*/\sigma)/w_k \propto \operatorname{arsinh}(\lambda d_k)/d_k$ is strictly decreasing in d_k. Both normalized vectors sum to 1 and share the same monotone ordering, so their ratio crosses 1 once; hence w strictly majorizes ε^*/σ whenever the d_k are not all equal. Strict convexity of $\sum u_k^2$ yields $\operatorname{Var}(\varepsilon^*) < \sigma^2 \operatorname{Var}(w)$. Pointwise $\cosh x - 1 > x^2/2$ off zero gives $C_*(\sigma) > C_Q(\sigma)$. Finally, expanding $\operatorname{arsinh}(\lambda/a_k) = \ln(2\lambda/a_k) + O(\lambda^{-2})$ yields $\sigma = M\ln(2\lambda) - \sum \ln a_k + O(\lambda^{-2})$, giving (20) and $\chi_k \to 1/M$. □

Table 1. Four-channel deterministic equilibrium for depths $a = (1, 2.5, 6, 12)$ (ceiling $\ln 12 = 2.4849$). Under hyperbolic cost, the gap bends beneath the ceiling while burden climbs exponentially and marginal shares equalize to 0.25. Under quadratic homeostasis, the gap grows linearly without bound and shares stay frozen at 0.606/0.051.

Skew σ	RS gap $\varepsilon_1^* - \varepsilon_4^*$	RS burden C_*	Quad. gap	Quad. burden C_Q	RS share (shallow / deep)
0.5	0.276	0.076	0.278	0.076	0.597 / 0.052
1.0	0.541	0.309	0.556	0.303	0.571 / 0.056
2.0	1.013	1.301	1.111	1.212	0.496 / 0.070
4.0	1.692	6.079	2.222	4.848	0.373 / 0.111
8.0	2.316	35.94	4.444	19.39	0.276 / 0.202
16.0	2.481	378.9	8.889	77.58	0.251 / 0.249
24.0	2.485	2,934	13.33	174.5	0.250 / 0.250

Table 1 and Figure 2(a) show the qualitative split cleanly: shallow channels buffer light load until $\lambda \approx a_k$, exhausting in order of depth. Once the finite buffer $\sum_k \ln(a_{\max}/a_k)$ is spent, every channel becomes equally stiff and takes an equal share $1/M$ of further skew, while each added unit of skew multiplies total burden by $e^{1/M}$.

Remark 6 (The clock-readout fork)**.** At the equilibrium (17), the log-ratios ε_k^* are strictly distinct for heterogeneous depths, while the marginal burdens $a_k \sinh \varepsilon_k^* = \lambda$ are *identical* across all channels. Consequently:

- Under Premise 1 ($\theta_k = \theta_0 + v\varepsilon_k$), nonzero skew strictly separates channel paces up to the finite variance ceiling $v^2 \operatorname{Var}_k(\ln a_k)$.
- Under a marginal-burden clock ($\theta_k = \theta_0 + c\, a_k \sinh \varepsilon_k$), every channel keeps the *exact same pace* $\theta_0 + c\lambda$ at equilibrium even at $\sigma \neq 0$.

This fork is not a defect; it is a sharp experimental discriminator (Section 9). Even under the marginal-burden readout, the log-ratios themselves still obey (18)–(21).

7 Finite-Temperature Fluctuations: Freezing and Variance Reversal

Deterministic minimization fixes setpoints, not fluctuations. Under Premise 4, we now evaluate the full Gibbs ensemble on $M \geq 2$ heterogeneous accounts under two natural constraints: the *fixed-total (hard-conditioned) ensemble* conditioning $\prod_k e^{-a_k \cosh X_k}$ on $\sum_k X_k = s$, and the *mean-total (tilted) ensemble* of independent accounts proportional to $e^{-a_k \cosh x + \ell x}$ with common tilt ℓ chosen so $\sum_k \mathbb{E}_\ell[X_k] = s$.

7.1 Exact solution for two accounts at every fixed skew

Theorem 7 (Exact two-account conditional law)**.** *Let two accounts with stiffnesses $a, b > 0$ carry joint density proportional to $e^{-a\cosh x_a - b\cosh x_b}$ on $\mathbb{R}^2$. Conditional on fixed total skew*

$X_a + X_b = s$, *define*

$$R(s) := \sqrt{a^2 + b^2 + 2ab\cosh s}, \qquad g_{ab}(s) := \ln\frac{a + be^s}{b + ae^s}. \tag{22}$$

Then the exact conditional law is

$$X_a = \frac{s + g_{ab}(s)}{2} + Y, \qquad X_b = \frac{s - g_{ab}(s)}{2} - Y, \qquad Y \sim p_{R(s)}, \tag{23}$$

where $p_{R(s)}$ is the symmetric single-account cosh-Gibbs density (8) *of effective stiffness $R(s)$. For $0 < a < b$ and $s > 0$:*

1. *The exact mean gap $\mathbb{E}[X_a - X_b \mid s] = g_{ab}(s)$ is strictly increasing with derivative $g'_{ab}(s) = (b^2 - a^2)/R(s)^2$, bounded strictly below both the universal cap and the exact quadratic gap:*

$$0 \;<\; g_{ab}(s) \;<\; \min\Big(\ln\frac{b}{a},\ \frac{b-a}{b+a}\,s\Big), \qquad \lim_{s\to+\infty} g_{ab}(s) = \ln\frac{b}{a}. \tag{24}$$

2. *Both marginal variances equal $V(R(s))$ and strictly decrease as $|s|$ grows, freezing exponentially as $R(s) \sim \sqrt{ab}\,e^{|s|/2}$.*

3. *For uniform subsystem selection under Premise 1, the exact signed centered coherence is $H_{\text{pool}}(q \mid s) = \cos(qg_{ab}(s)/2)\,H_{R(s)}(q)$.*

Proof. Substituting $x_b = s - x_a$ into $a\cosh x_a + b\cosh x_b$ yields $\frac{1}{2}[(a + be^{-s})e^{x_a} + (a + be^s)e^{-x_a}]$. Recentering at $x_0 = \frac{1}{2}\ln[(a + be^s)/(a + be^{-s})] = \frac{1}{2}(s + g_{ab}(s))$ transforms the action identically into $R(s)\cosh(x_a - x_0)$, since $(a + be^s)(a + be^{-s}) = R(s)^2$. Symmetry of $p_{R(s)}$ gives the means, medians, and marginal variances $V(R(s))$. Differentiating $g_{ab}(s)$ gives $g'_{ab}(s) = (b^2 - a^2)/R(s)^2 > 0$, which is strictly decreasing for $s > 0$ from its initial value $(b - a)/(b + a)$, proving (24). Finally, $V'(r) = -\operatorname{Cov}_r(X^2, \cosh X) < 0$ (by the same monotone-covariance argument as Theorem 2) implies strict narrowing in $|s|$. □

7.2 Generalization to arbitrary M and total-variance reversal

The same two-part mechanism—strictly separating means paired with shrinking individual fluctuations—extends to arbitrary $M \geq 2$ in both ensembles:

Theorem 8 (All-M narrowing and mean separation)**.** *For any $M \geq 2$ accounts with positive stiffnesses $a_1, \ldots, a_M$:*

1. ***Common tilt:*** *Every individual variance $v_a(\ell) = \partial_\ell^2 \ln[2K_\ell(a)]$ strictly decreases in $|\ell|$, with $v_a(\ell) = |\ell|^{-1} + O(\ell^{-2})$ as $|\ell| \to \infty$. Whenever $a_i < a_j$, the mean gap $m_{a_i}(\ell) - m_{a_j}(\ell)$ strictly increases in ℓ and tends to $\ln(a_j/a_i)$ as $\ell \to +\infty$.*

2. ***Fixed total:*** *Whenever $a_i < a_j$, the conditional mean gap $\mathbb{E}[X_i - X_j \mid \sum_k X_k = s]$ strictly increases in s and tends to $\ln(a_j/a_i)$ as $s \to +\infty$, while the conditional covariance concentrates as $\operatorname{Cov}(X \mid s) = Q^{-1}(I - \mathbf{1}\mathbf{1}^T/M) + O(Q^{-2})$ with $Q = (G/2)e^{|s|/M}$.*

Proof. For a tilted account, taking two independent copies X, X' and writing $U = (X + X')/2$, $D = (X - X')/2$ gives $D \mid U = u \sim p_{2a\cosh u}$, so $v_a(\ell) = 2\,\mathbb{E}_\ell[V(2a\cosh U)]$. Because the density of $|U|$ is proportional to $K_0(2a\cosh u)\cosh(2\ell u)$, raising $|\ell|$ increases the likelihood ratio strictly in u, strictly lowering the expectation of the decreasing function $V(2a\cosh u)$. For large order $\ell \to +\infty$ at fixed $a > 0$, the uniform large-order Bessel expansion gives $K_\ell(a) = \sqrt{\pi/(2\ell)}\,(2\ell/(ea))^\ell\,[1 + O(\ell^{-1})]$ [10], so $\ln[2K_\ell(a)] = \ell\ln(2\ell/a) - \ell - \frac{1}{2}\ln\ell + \text{const} + O(\ell^{-1})$; differentiating twice in ℓ (justified by analyticity in a sector around the positive real axis) gives $m_a(\ell) = \ln(2\ell/a) + O(\ell^{-1})$ and $v_a(\ell) = \ell^{-1} + O(\ell^{-2})$, whence $m_{a_i}(\ell) - m_{a_j}(\ell) \to \ln(a_j/a_i)$. For strict monotonicity of the tilted mean gap, conditioning on $S = X_i + X_j$ cancels the tilt and gives $m_{a_i}(\ell) - m_{a_j}(\ell) = \mathbb{E}_\ell[g_{a_ia_j}(S)]$, whose ℓ-derivative is $\mathrm{Cov}_\ell(g_{a_ia_j}(S), S) > 0$.

For fixed total at $M > 2$, write h for the sum density of the remaining $M - 2$ accounts and $\alpha = (\sum_{\text{rest}} a_k^{-1})^{-1}$. Each factor $e^{-a_k\cosh x + a_k x^2/2}$ is log-concave, so Prékopa's marginalization theorem [13] implies $e^{\alpha t^2/2}h(t)$ is log-concave; thus $h(s_2 - t)/h(s_1 - t)$ is strictly increasing in t for $s_2 > s_1$, forcing strict monotonicity of $\mathbb{E}[g_{a_ia_j}(T) \mid s]$ in s (where $T = X_i + X_j$). For the $s \to +\infty$ limit and covariance, substitute $X_k = s/M + \ln(G/a_k) + y_k$ on the $(M-1)$-dimensional hyperplane $H_0 = \{\sum_{k=1}^M y_k = 0\}$. The action becomes

$$\Phi_s(y) = Q\sum_{k=1}^M e^{y_k} + \frac{1}{4Q}\sum_{k=1}^M a_k^2 e^{-y_k},$$

which is strictly convex on H_0 with gradient $\nabla_{H_0}\Phi_s(0) = O(Q^{-1})$ and Hessian $Q\,\mathrm{diag}(e^{y_k})|_{H_0} + O(Q^{-1})$. Its unique minimizer $y^*(s)$ therefore satisfies $\|y^*(s)\| = O(Q^{-2})$, and Laplace's method on H_0 yields $\mathbb{E}[y \mid s] = O(Q^{-1})$ (so $\mathbb{E}[X_i - X_j \mid s] = \ln(a_j/a_i) + O(Q^{-1})$) together with

$$\mathrm{Cov}(X \mid s) = \mathrm{Cov}(y \mid s) = Q^{-1}P_{H_0} + O(Q^{-2}) = Q^{-1}\left(I - \frac{\mathbf{1}\mathbf{1}^T}{M}\right) + O(Q^{-2}).$$

□

Now consider the law of total variance across uniformly sampled subsystems—the operational dispersion measured when standardized phase-rate fluctuations are aggregated across coupled channels without conditioning on channel identity:

$$T(s) = \mathrm{Var}(X_I \mid s) = \underbrace{\frac{1}{M}\sum_{k=1}^M \mathrm{Var}(X_k \mid s)}_{A_{\text{within}}(s)} + \underbrace{\mathrm{Var}_k(\mathbb{E}[X_k \mid s])}_{B(s)}. \tag{25}$$

Because $B(s)$ rises while $A_{\text{within}}(s)$ falls, their sum $T(s)$ is *not* guaranteed to increase with skew.

Theorem 9 (Stress-induced freezing and total-variance reversal)**.** *In both the fixed-total and common-tilt ensembles, unresolved skew can strictly* reduce *total pooled variance T even while strictly separating subsystem means. Specifically, for $a = 1, b = 2$:*

- *At fixed total $s = 0$, $T(0) = V(3) > 2/7$; at $s = \ln 512$, $R(s) > 32$ and $g_{12}(s) < \ln 2 < 1$, so $T(s) < 1/32 + 1/4 = 9/32 < 2/7 < T(0)$ analytically. By direct numerical quadrature (see Computational Reproducibility below), raising s from 0 to 2 raises B from 0 to 0.067361 while dropping A_{within} from 0.291274 to 0.202919, lowering total variance from 0.291274 to 0.270280.*

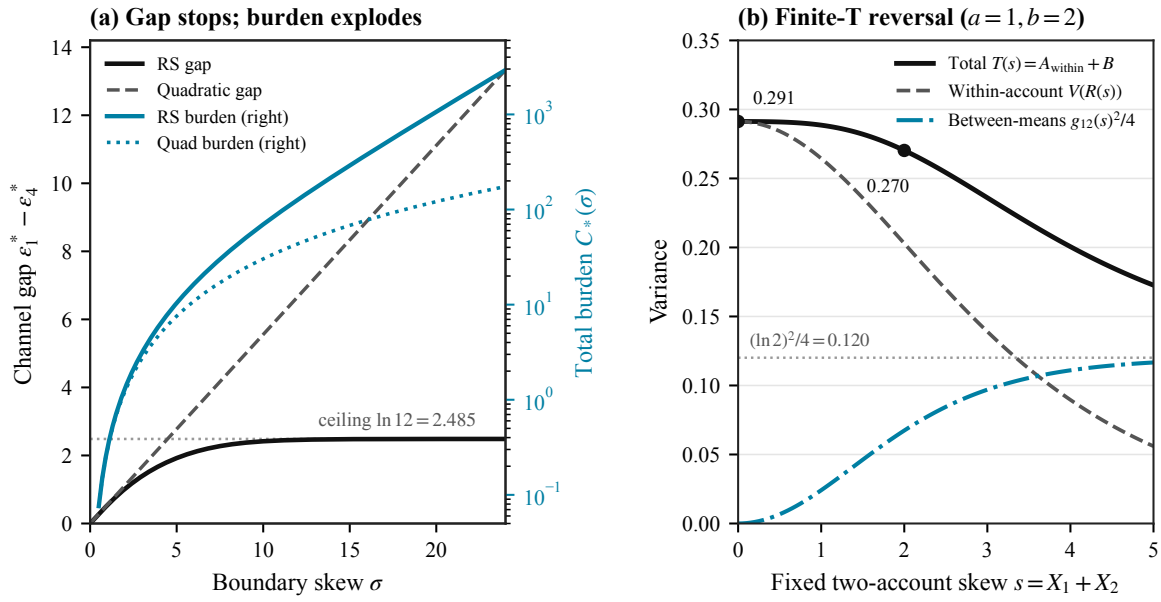


Figure 2. (a) Deterministic ceiling and exponential burden. Four channels of depths $(1, 2.5, 6, 12)$: the RS shallow–deep gap bends beneath $\ln 12 = 2.485$ while total burden climbs exponentially to 2,934; quadratic homeostasis yields an unbounded linear gap (13.3) and parabolic burden (175). **(b) Exact finite-temperature variance reversal ($a = 1, b = 2$).** Raising fixed skew s separates subsystem means (B rises toward $(\ln 2)^2/4 = 0.120$) while freezing within-account fluctuations ($V(R(s))$ drops sharply), pulling total pooled variance $T(s)$ *down* from 0.291 to 0.270 at $s = 2$.

- *Under common tilt* $\ell = 0 \to 2$ *(mean total* $0 \to 2.0347$*), quadrature gives* $B : 0 \to 0.058450$ *while* $A_{\text{within}} : 0.572855 \to 0.409813$*, lowering* T *from* 0.572855 *to* 0.468263*.*
- *By contrast, for sharper contrast* $(a = 1, b = 9)$*, the limiting between-mean variance* $(\ln 9)^2/4 \approx 1.207$ *exceeds both zero-skew baselines* ($V(10) < 0.1$ *and* $[V(1) + V(9)]/2 < 5/9$)*, so* T *experiences a net increase* ($T(\infty) > T(0)$) *at large skew.*

This reversal (Figure 2(b)) has direct physical and experimental meaning. Measuring only raw pooled variability can mistake stress-induced hyper-rigidity (two channels frozen around displaced setpoints) for increased stability. A valid test of human coherence must decompose variability into *between-channel mean separation* and *within-channel fluctuation.*

8 Time, Living Drive, Reserve Exhaustion, and Outside Rhythms

8.1 Still, skewed, and alive

If zero skew and zero spread maximize $|W|$, what distinguishes a coherent living person from a dead rock? Let bond b's log-flow vary across the ticks of a repeating window, with window sum $S_b = \sum_{t \in \text{window}} \varepsilon_b(t)$. At the close of the n-th window, the accumulated phase is $n(\text{window length} \cdot \theta_0 + \nu S_b)$, so the dispersion bracket (5) applies verbatim with n in place of t and S_b in place of ε_b. Balanced excursions inside a window leave $|W| = 1$ at every window

close; only differences between window sums accumulate, and they grow as n^2.

Three independent window coordinates classify every trajectory: total activity $\mathscr{A} = \sum_b \sum_t |\varepsilon_b(t)|$, net window skew σ_W, and window-sum spread D_W.

1. **Stillness ($\mathscr{A} = 0$, $\sigma_W = 0$, $D_W = 0$):** Every ratio is 1, burden is 0, and $|W| = 1$. Within the broader Recognition Boundary Theory framework [16], an attentive recognizer whose own postings enter the scope it registers cannot complete its registry permanently, keeping $\mathscr{A} > 0$ for a living boundary; on the bond ledger alone, $\mathscr{A} > 0$ serves as the operational condition separating living coherence from stillness.
2. **Skewed or spread agitation ($\mathscr{A} > 0$, $\sigma_W \neq 0$ or $D_W > 0$):** Cost sits strictly above the even floor, paces separate, and standing skew drains reserves.
3. **Living human coherence ($\mathscr{A} > 0$, $\sigma_W = 0$, $D_W = 0$):** Active open exchange on closed loops at uniform pace, maintaining constant positive standing burden $2J(g) > 0$ per equilibrated pair while net window skew and spread stay zero.

8.2 Logarithmic reserve exhaustion and eight-tick window order

Theorem 10 (Logarithmic reserve exhaustion)**.** *Assume an uncompensated skew step $s \neq 0$ accumulates linearly on a bond each window, $\varepsilon_n = ns$.*

1. ***Instantaneous standing-burden ceiling:*** *The standing burden* $\cosh(ns) - 1$ *after n windows exceeds a positive capacity $E > 0$ if and only if*

$$n \;>\; n^*(E, s) \;:=\; \frac{\operatorname{arcosh}(1 + E)}{|s|}. \tag{26}$$

2. ***Cumulative-burden depletion:*** *The cumulative cost $\sum_{j=1}^{n}(\cosh(js) - 1)$ paid over n windows exceeds a finite stock $E > 0$ at $n^*_{\mathrm{cum}}(E, s) = \frac{1}{|s|}\ln[2E(1 - e^{-|s|})] + O(1)$ as $E \to \infty$.*

Proof. Part (1) follows immediately from cosh being even and strictly increasing on $[0, \infty)$. For Part (2), summing the geometric series gives $\sum_{j=1}^{n}(\cosh(js) - 1) = \frac{e^{(n+1)|s|} - e^{|s|}}{2(e^{|s|}-1)} + \frac{1-e^{-n|s|}}{2(e^{|s|}-1)} - n$, whose leading term is $\frac{e^{n|s|}}{2(1-e^{-|s|})}$; inverting against E yields the stated logarithmic scaling. □

Under both readings (standing capacity or cumulative stock), doubling a large reserve buys only $\ln 2/|s|$ additional windows under hyperbolic cost, whereas a quadratic penalty gives power-law endurance: $n^*_Q = \sqrt{2E}/|s|$ for standing capacity and $n^*_{Q,\mathrm{cum}} \sim (6E/s^2)^{1/3}$ for cumulative depletion. At $s = 0.5$ under the standing-capacity reading, raising E from 100 to 10,000 extends endurance from 28.3 to 282.8 windows under a quadratic penalty, but only from 10.6 to 19.8 windows under J.

For a living active boundary ($\mathscr{A} > 0$, $\sigma_W = 0$) cycling over the fundamental eight-tick window with fixed step amplitude $\pm\alpha$ (four +, four −, giving $\binom{8}{4} = 70$ balanced orders), exhaustive enumeration solves the discrete scheduling problem directly: every neutral active window has at least 2 cyclic sign switches and running-balance burden at least $4(\cosh\alpha - 1)$; 16

orders attain minimum burden (keeping running balance inside $\{-\alpha, 0, \alpha\}$); 6 of those have zero mean outstanding balance; and exactly two—the palindromic cycles ABBA · ABBA and BAAB · BAAB—minimize cyclic switches (4 switches, half of ABAB · ABAB's 8, with zero standing bias against ABAB's bias of $\alpha/2$).

8.3 What a zero-net-flow outside rhythm can and cannot do

Two immediate invariances frame external pacing: if a drive adds an independent cost term and does not enter the turn-rate map, $W(t)$ is unchanged; and adding a uniform frequency shift $\delta\theta$ to every channel rotates $\arg W(t)$ without changing $|W(t)|$. The substantive constraints come from boundary conservation and strong convexity of $J_{\log}$:

Theorem 11 (Trade-off of a zero-net-flow outside rhythm)**.** *Let an external periodic drive act on a composite boundary of heterogeneous depths $a_1, \dots, a_M > 0$ carrying unresolved boundary skew $\sigma \neq 0$.*

1. ***Skew invariance under zero-net-flow drives:*** *By Theorem 3, a drive changes σ_W only by the net log-flow on bonds it shares with the boundary; any zero-net-flow drive leaves σ_W untouched.*
2. ***Strict holding excess:*** *Under Premise 4, any allocation ε with $\sum_k \varepsilon_k = \sigma$ obeys*

$$C(\varepsilon) - C_*(\sigma) \;\geq\; \frac{1}{2}\sum_{k=1}^{M} a_k(\varepsilon_k - \varepsilon_k^*)^2. \tag{27}$$

In particular, the aligned zero-spread allocation $\varepsilon_k = \sigma/M$ is feasible at any skew, has cost $C_{\text{hold}} = (\sum_k a_k)(\cosh(\sigma/M) - 1)$, is non-stationary because $a_k \sinh(\sigma/M)$ varies across depths, and requires strictly positive holding excess

$$C_{\text{hold}} - C_*(\sigma) \;\geq\; \frac{1}{2}\, a_{\min}\, M\, \operatorname{Var}_k(\varepsilon^*) \;>\; 0. \tag{28}$$

Proof. Part (1) is an immediate consequence of (13). For Part (2), because $\cosh''(u) = \cosh u \geq 1$ everywhere, the tangent quadratic bound from Theorem 1 gives $a_k[J_{\log}(\varepsilon_k) - J_{\log}(\varepsilon_k^*) - \sinh(\varepsilon_k^*)(\varepsilon_k - \varepsilon_k^*)] \geq \frac{1}{2}a_k(\varepsilon_k - \varepsilon_k^*)^2$. Summing over k, the linear term equals $\lambda \sum_k(\varepsilon_k - \varepsilon_k^*) = 0$ on the constraint, proving (27). Evaluating at $\varepsilon_k = \sigma/M$ gives $\sum_k(\sigma/M - \varepsilon_k^*)^2 = M \operatorname{Var}_k(\varepsilon^*)$ and (28). □

A zero-net-flow outside rhythm therefore faces an exact static trade-off: *spread and excess burden cannot both vanish while $\sigma \neq 0$.* With depths $(1, 2.5, 6, 12)$ at $\sigma = 3$, the free separated state costs 3.14 while holding alignment costs 6.34—more than double. Theorem 11 is a static variational inequality; adding any cost-decreasing interior relaxation (such as constrained gradient flow $\dot{\varepsilon} = -\Pi_{\sum=0}\nabla C(\varepsilon)$) implies that releasing the external drive relaxes a skewed boundary back to the unique separated minimum ε^*, whereas a balanced boundary ($\sigma = 0$) stays aligned at zero excess cost.

9 Prospective Experimental Falsifiers

No physiological data were fitted or scored in deriving these laws. To keep the framework strictly accountable to nature, we specify three prospective, noninvasive experimental protocols targeting distinct links in the derivation, together with honest power bounds against the quadratic rival.

9.1 Protocol A: Stiffness-free conditional energy-split test

Choose a single signed physiological exchange ratio with an individually calibrated, preregistered neutral baseline r_0—for instance, the signed log ratio of inspiratory to expiratory duration $X = \ln[(T_{\text{in}}/T_{\text{out}})/r_0]$ from calibrated airflow (calibrating r_0 per participant avoids confounding the known resting I:E asymmetry of roughly $1:1.5$–$1:2$ with ledger skew; this physiological mapping is a candidate realization outside P1–P4). For each of $N = 167$ independently sampled participants, record one prospectively selected draw in each of two matched, temporally separated blocks in the *large-excursion regime*, yielding (X_1, X_2) at shared unknown personal stiffness $a > 0$.

Transform to canonical cost $C_j = \cosh X_j - 1$ ($j = 1, 2$), sum $R = C_1 + C_2$, and split fraction $U = C_1/R \in (0, 1)$. Under (8), the marginal density of $C > 0$ is proportional to $e^{-aC}/\sqrt{C(C+2)}$. Conditioning on $R = r$ cancels the unknown stiffness a *identically*, leaving the stiffness-free conditional density on $(0, 1)$:

$$f_r(u) \;\propto\; \big[u(1-u)(2+ru)(2+r(1-u))\big]^{-1/2}. \tag{29}$$

Let $P = F_R(U)$ be the conditional probability integral transform. Under the compound null (independent matched blocks, calibrated r_0, shared a, and cosh-Gibbs law), $P \sim \text{Uniform}(0, 1)$ across the entire cohort even if every participant has a different stiffness a. Under a quadratic cost in the same X coordinates, (29) is multiplied by $\exp[-\frac{a}{2}(\text{arcosh}^2(1+ru) + \text{arcosh}^2(1 + r(1-u)))]$ (Figure 3(b)).

Decision rule and power against the quadratic rival: Using Massart's conservative distribution-free DKW bound [14], reject compatibility if $\sup_{v\in[0,1]} |\widehat{F}_P(v) - v| > \sqrt{\ln(40)/(2 \cdot 167)} = 0.105093$ (guaranteed size ≤ 0.05; power ≥ 0.90 against any alternative at sup-norm PIT distance ≥ 0.20). Crucially, because $\cosh x - 1 \approx x^2/2$ near $x = 0$, quiet resting fluctuations ($R \le 1$) yield tiny quadratic-decoy PIT distances (0.001–0.023 for $a \in [0.5, 5]$) and cannot separate the models. Discrimination requires large excursions: at $R = 4$, the quadratic decoy's PIT distance rises from 0.038 ($a = 1$) to 0.166 ($a = 5$), and at $R = 10$ it reaches 0.181 ($a = 2$) and 0.289 ($a = 5$). Protocol A must therefore be executed under large-excursion perturbations (conditioning on $R \ge 4$), where $N = 167$ achieves high power against the quadratic rival.

9.2 Protocol B: Calibrated two-clock exact median sign test

Acquire two independently instrumented physiological channels simultaneously—for example, cardiac cycle timing from ECG plus an independent pulse-wave channel, and respiratory timing from calibrated airflow plus a separate belt transducer (simultaneous resting ECG/respiration

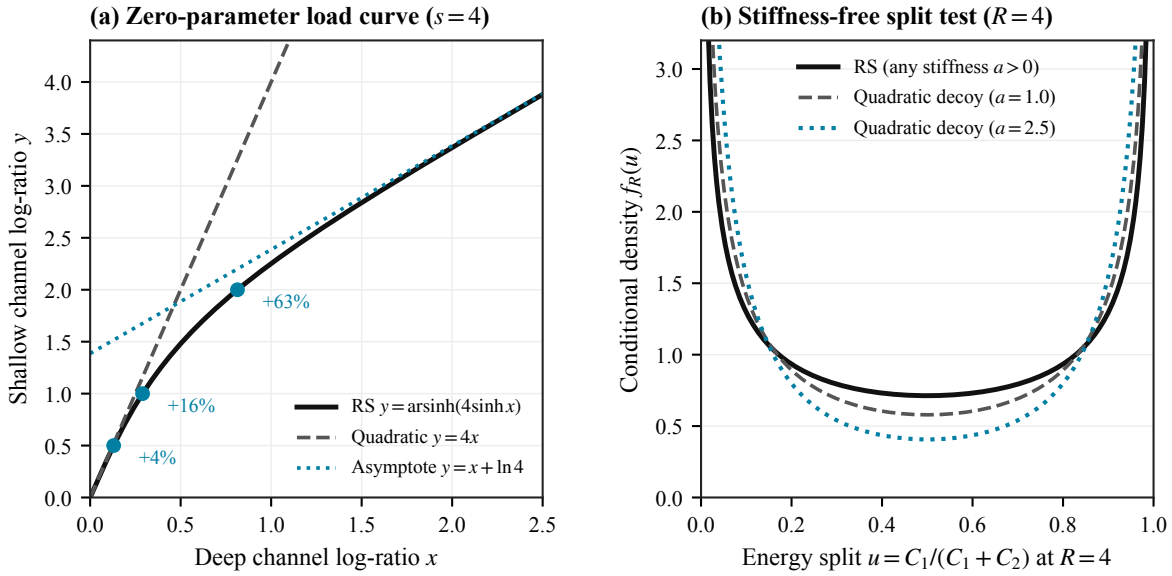


Figure 3. (a) Zero-parameter nonlinear bend of the graded-load curve ($s = 4$). Reading the initial slope s at light load fixes the entire curve $y = \operatorname{arsinh}(s \sinh x)$ and heavy-load offset $\ln s$ with no further free parameters. Markers show +4%, +16%, and +63% separation from the quadratic straight line $y = 4x$ at shallow log-ratios 0.5, 1.0, and 2.0. **(b) Stiffness-free conditional energy-split density ($R = 4$).** Under the hyperbolic law, the density $f_R(u)$ is identical for every stiffness $a > 0$ (solid), whereas the quadratic decoy (dashed/dotted) depends on a and tilts weight toward the center.

acquisition is standard [15]). Define two signed candidate coordinates (X_a, X_b) relative to pre-registered neutral baselines, calibrate only their stiffness ratio b/a from a separate light-load cohort (so no absolute stiffness or temperature enters), and read independently instrumented phase shifts $Z_i = (\Delta\phi_i - \theta_{0i}t)/(c_i t)$ over the next short fixed lag under strong controlled load.

At total $s = X_a + X_b$, Theorem 7 predicts that the conditional median of $D = Z_a - Z_b$ is $g_{ab}(s) = \ln[(a + be^s)/(b + ae^s)]$, whereas quadratic homeostasis predicts $(b - a)s/(b + a)$.

Decision rule and power against the quadratic rival: Across $N = 17$ independent participants (one pre-registered high-load epoch per person), count positive signs of $\operatorname{sgn}(s)[D - g_{ab}(s)]$. Under the continuous calibrated null (Premise 1, calibrated b/a, known gains c_i, and hard total s), the count is Binomial$(17, 1/2)$ even when participants have different totals s. Reject at 0–4 or 13–17 positives (exact two-sided size 0.04904; power 0.9013 at sign probability 0.85). Computing power directly against the quadratic rival shows why strong load is essential: at mild load $s = \ln 4$ with $a : b = 1 : 4$, $g_{\text{hyp}} = 0.754$ vs. $g_{\text{quad}} = 0.832$ against conditional standard deviation $2/\sqrt{5} \approx 0.894$, giving sign probability 0.535 (requiring $N \gtrsim 2{,}170$ for 90% power). By contrast, in the strong-load regime $s = 4.0$ ($a : b = 1 : 4$), $g_{\text{hyp}} = 1.320$ vs. $g_{\text{quad}} = 2.400$ yields sign probability 0.886 (90% power reached at $N = 13 \leq 17$), and at $a : b = 1 : 9$, $s = 4.0$, sign probability reaches 0.966 ($N = 7$).

Precision note on direct Fourier detection: Detecting the single-account negative Bessel lobe $H_1(3.5) = -0.01116$ directly from independent bounded cosine readings requires a 95% Hoeffding half-width below 0.01116, i.e. $n \gtrsim 59{,}231$ independent readings at known gain v. High-load conditional protocols A and B therefore achieve decisive discrimination with orders

of magnitude fewer participants.

9.3 Protocol C: Graded-load channel curve, clock fork, and rhythm release

Load a person in graded physiological steps while recording two channels of unequal depth.

1. **Nonlinear bend with zero post-slope parameters:** Plot the shallow channel's log-ratio y against the deep channel's log-ratio x. Equation (21) predicts $y = \operatorname{arsinh}(s \sinh x)$: once $s = a_k/a_j$ is estimated from the initial light-load slope, the entire nonlinear bend and heavy-load offset $\ln s$ are fixed with no further free parameters (Figure 3(a)). At finite temperature, Theorem 7 shows that conditional observations scatter around the exact mean gap $g_{ab}(s)$ with variance $V(R(s))$ that shrinks exponentially at high load, so the deterministic curve becomes sharper precisely where it diverges from linearity. For $s = 4$, the hyperbolic and quadratic curves stay within 4% below $y = 0.5$, separate by 16% at $y = 1$, and separate by 63% at $y = 2$, so testing requires loads moving the shallow channel by at least a factor of e.
2. **Deciding the clock fork:** Conditioned on confirming nonzero heterogeneous log-ratio load in step (1) ($\sigma \neq 0$ and $s \neq 1$, ruling out balance or homogeneous depths), measure how far each channel's pace shifts across the load steps. Unequal pace shifts tracking ε_k^* confirm Premise 1; a uniform shift across channels confirms the marginal-burden readout of Remark 6.
3. **Rhythm release:** Apply a zero-net-flow external pacing rhythm (such as paced breathing) during unresolved load and then release it. Under cost-decreasing interior relaxation, Theorem 11 predicts return to the separated settled paces when $\sigma \neq 0$, versus persistence when $\sigma = 0$.

10 What Is Established, What Is Identified, and What Remains Open

Table 2 separates the proved mathematics from the working physical identifications and the open scientific questions.

Remark 12 (Relation to boundary-record purity)**.** The separate boundary-record theory of coupled finite recognition instruments [16] studies the purity of conditional present records rather than the phase average $W(t)$ directly. Connecting conditional-record purification across shared interactions to autonomic timing or social isolation requires an additional physical bridge and is kept distinct from the bond-ledger theorems proved here.

Table 2. Exact epistemological boundary of the derivation.

Status	Content
Established mathematics	Canonical cost $J(x) = \frac{1}{2}(x + x^{-1}) - 1$ and d'Alembert identity [1, 2]; refutation of $W = e^{-C}$ and two-sided turn-rate dispersion bracket; Thrift Bracket (Theorem 1); Bessel envelope $K_{iq}(a)/K_0(a)$, $(a + \frac{1}{2})^{-1} < V(a) < a^{-1}$, and universal platykurtosis $c_4 < 0$ (Theorem 2); Boundary Charge Law (Theorem 3); Pair Factorization, shared-bond symmetry, coherence $\lvert\cos(v\sigma t/2)\rvert$, and equilibration saving (Theorem 4); Heterogeneous Channel Law, $\ln(a_k/a_j)$ ceiling, global majorization vs. quadratic, exponential burden, and $y = \operatorname{arsinh}(s \sinh x)$ (Theorem 5); Exact two-account conditional law, all-M narrowing/separation, and total-variance reversal (Theorems 7–9); Logarithmic reserve exhaustion (Theorem 10); Zero-net-flow rhythm holding excess (Theorem 11).
Working identifications	Premise 1 (turn rate reads log-ratio with common linear gain v); Premise 2 (a human is a composite boundary with unequal series depths a_k); Premise 3 (boundary bond ensemble); Premise 4 (least-burden interior and flat log-ratio cosh-Gibbs measure); reading the ledger's capacity/stock as an exhaustible physiological reserve; candidate respiratory/cardiac coordinate maps in Section 9; cost-decreasing relaxation after drive release.
Open scientific frontiers	(1) Mapping specific human organs and biomarkers to bonds and depths a_k; (2) deriving the clock gain v and linking the fundamental recognition tick to neural, cardiac, and respiratory periods in seconds; (3) resolving the log-ratio vs. marginal-burden clock fork experimentally; (4) deriving interior relaxation dynamics and determining whether living dynamics conserves total bond flow or only boundary cut flow; and (5) the dual-aspect bridge explaining why balanced exchange at one pace is felt as clarity and ease.

11 Conclusion

Human coherence need be neither a vague metaphor nor a fragile quantum state. On the recognition ledger, under four explicit working identifications, it is a precise, falsifiable physical regime: active exchange across an open boundary whose books close ($\sigma = 0$) and whose channels turn at one pace ($D = 0$).

Total cost does not break coherence; wasted cost above even exchange does. Between two people, skew and throughput multiply in cost while coherence reads skew alone, and shared-bond reciprocity gives both parties the exact same burden and coherence curve. Inside one person, unresolved skew concentrates onto the shallowest channels first, hits a universal log-ratio ceiling $\ln(a_k/a_j)$ while total burden grows exponentially, and at finite temperature can freeze within-channel variability enough to pull total pooled variance down even as setpoints tear apart. Zero-net-flow external rhythms can hold alignment only at a continuing excess burden while skew remains open. What remains is experimental: measuring which biological clocks read which ledger ratios, and testing the high-excursion energy-split, calibrated sign, and graded-load laws directly on human physiology.

Computational reproducibility

All numerical values in Section 4, Table 1, Theorem 9, Section 8, Section 9, and Figures 1–3 were computed in double precision using adaptive Gauss–Kronrod quadrature (relative tolerance 10^{-12}) for $K_0(a)$, $K_{iq}(a)$, $V(a)$, $m_4(a)$, and conditional PIT distributions, together with safeguarded Newton iteration (tolerance 10^{-14}) for the Lagrange multiplier $\lambda(\sigma)$ in (17). Standalone Python scripts reproducing every table entry and figure are archived alongside the manuscript source.

References

[1] J. Washburn and M. Zlatanović, "Uniqueness of the Canonical Reciprocal Cost," *Mathematics* **14**(6) (2026), 935.

[2] J. Washburn, M. Zlatanović, and E. Allahyarov, "The d'Alembert Inevitability Theorem," *Mathematics* **14**(8) (2026), 1386.

[3] S. Pardo-Guerra, J. Washburn, and E. Allahyarov, "A Coherence Theorem for Conserved Comparison Ledgers: Structural Axioms Pin Down the Scale, the Cost, and the Ratio," *Mathematics* **14**(15) (2026), 2672.

[4] Y. Kuramoto, *Chemical Oscillations, Waves, and Turbulence*, Springer-Verlag, Berlin (1984).

[5] C. Schäfer, M. G. Rosenblum, J. Kurths, and H.-H. Abel, "Heartbeat synchronized with ventilation," *Nature* **392** (1998), 239–240.

[6] P. M. Lehrer and R. Gevirtz, "Heart rate variability biofeedback: how and why does it work?" *Frontiers in Psychology* **5** (2014), 756.

[7] P. Sterling, "Allostasis: a model of predictive regulation," *Physiology & Behavior* **106**(1) (2012), 5–15.

[8] F. W. J. Olver et al., *NIST Digital Library of Mathematical Functions*, §10.32, Integral Representations of Modified Bessel Functions, `https://dlmf.nist.gov/10.32#E9`.

[9] F. W. J. Olver et al., *NIST Digital Library of Mathematical Functions*, §10.40, Asymptotic Expansions for Large Argument, `https://dlmf.nist.gov/10.40#E2`.

[10] F. W. J. Olver et al., *NIST Digital Library of Mathematical Functions*, §10.41, Asymptotic Expansions for Large Order, `https://dlmf.nist.gov/10.41#E2`.

[11] F. W. J. Olver et al., *NIST Digital Library of Mathematical Functions*, §10.45, Functions of Imaginary Order, `https://dlmf.nist.gov/10.45`.

[12] R. B. Paris, "The zeros of the modified Bessel function $K_{iv}(x)$ of imaginary order," arXiv:2108.01447 (2021).

[13] A. Prékopa, "On logarithmic concave measures and functions," *Acta Scientiarum Mathematicarum (Szeged)* **34** (1973), 335–343.

[14] P. Massart, “The tight constant in the Dvoretzky–Kiefer–Wolfowitz inequality,” *Annals of Probability* **18**(3) (1990), 1269–1283.

[15] N. Iyengar, C. K. Peng, R. Morin, A. L. Goldberger, and L. A. Lipsitz, “Age-related alterations in the fractal scaling of cardiac interbeat interval dynamics,” *American Journal of Physiology* **271** (1996), R1078–R1084; PhysioNet Fantasia Database v1.0.0, `https://physionet.org/content/fantasia/1.0.0/`.

[16] J. Washburn, *Recognition Boundary Theory: How One Ledger Holds Many Perspectives*, Recognition Physics Institute (2026), DOI: 10.5281/zenodo.23706422.

[17] J. Washburn, *The Physical Moral Code of Reality: Boundary Locality, One-Subject Impartiality, Fourteen-Law Closure, and Empirical Boundaries on the Recognition Ledger*, Recognition Physics Institute (2026), DOI: 10.5281/zenodo.24413322.